Spacetime Wave

Solar Interferometer MVP

Mecklenburg-Vorpommern / Germany

Version: 2021-03-12

Author: Eckhard Kantz

Contact: mvp@wegalink.eu

Download:

https://wegalink.eu/spacetime_waves/doc/spacetime_wave_solar_interferometer.pdf

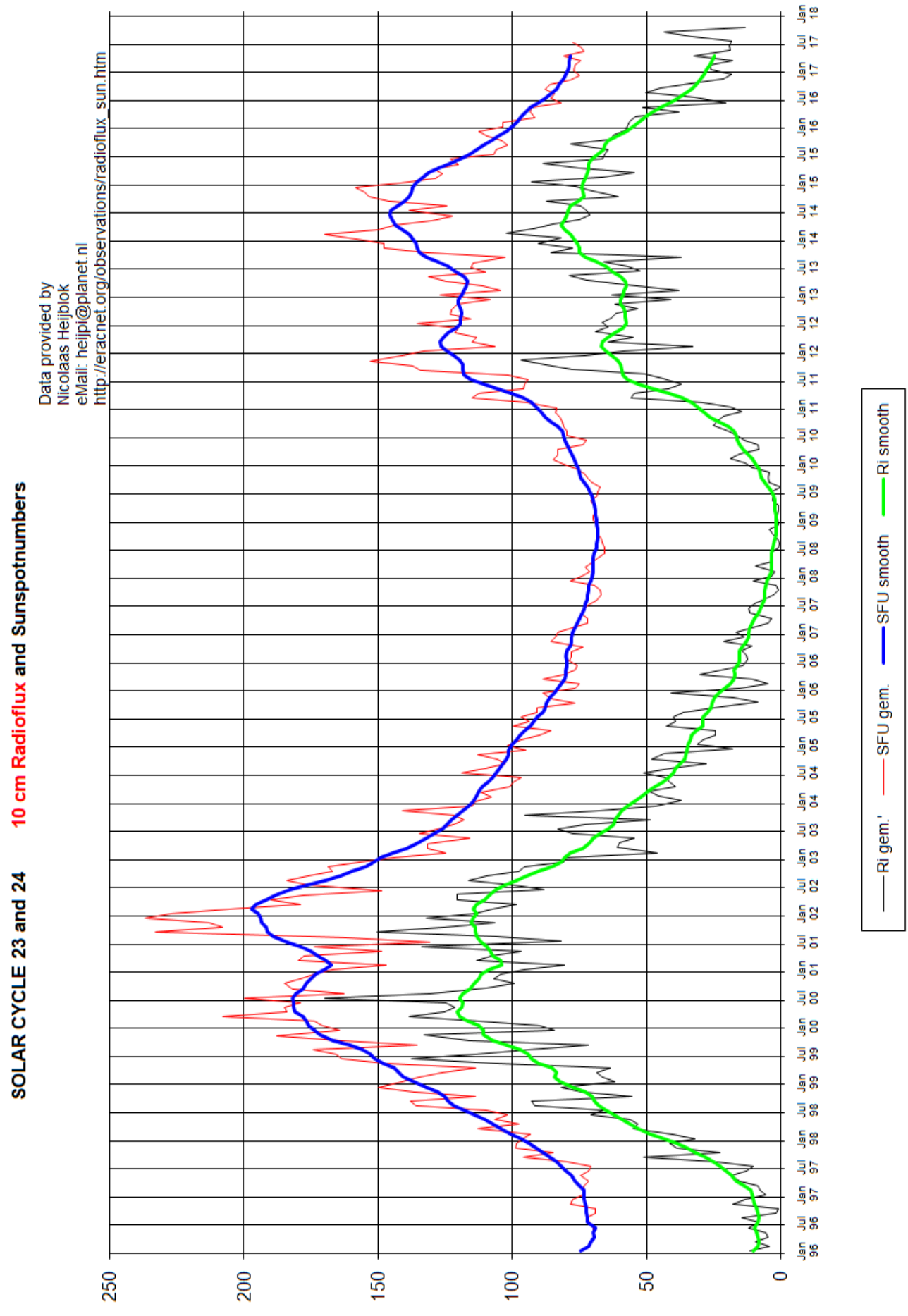
SOLAR CYCLE 23 and 24
10 cm Radioflux and Sunspotnumbers
Data provided by
Nicolaas Heijblok
eMail: heijbl@planet.nl
http://eracnet.org/observations/radioflux_sun.htm
250
200
150
100
50
0
Jan 96
Jul 96
Jan 97
Jul 97
Jan 98
Jul 98
Jan 99
Jul 99
Jan 00
Jul 00
Jan 01
Jul 01
Jan 02
Jul 02
Jan 03
Jul 03
Jan 04
Jul 04
Jan 05
Jul 05
Jan 06
Jul 06
Jan 07
Jul 07
Jan 08
Jul 08
Jan 09
Jul 09
Jan 10
Jul 10
Jan 11
Jul 11
Jan 12
Jul 12
Jan 13
Jul 13
Jan 14
Jul 14
Jan 15
Jul 15
Jan 16
Jul 16
Jan 17
Jul 17
Jan 18
Ri gem.'
SFU gem.
SFU smooth
Ri smooth

Objective

Our Lady Sun is a source of ever changing flow of energy. Until recently, it was only possible to observe energy streams radiated from the surface of the Sun by well known electromagnetic waves on all technically feasible frequencies as shown for example on the chart "**Solar Cycle 23 and 24 – 10 cm Radioflux and Sunspotnumbers**".

The confirmation of gravitational waves as postulated by Einstein, by recording data from two black holes collapsing to one black hole while loosing several solar masses and radiating the equivalent of the lost mass as gravitational waves, opens new opportunities.

This document describes a system that takes advantage of the *elasticity of our spacetime* which now has become available to measurement systems thanks to the successful detection of *gravitational waves*. Investigated waves could be called **spacetime waves**.

Theoretic assumptions

More than 100 years ago, Albert Einstein put his idea of the equivalence of mass and energy into his famous formula:

- $E = mc^2$

Before using that relationship, we consider the energy conversion processes in our Sun dependent on location inside the solar sphere and dependent on time:

- E(c,g,s,t)

where the parameters are chosen as follows:

c – direction from the Sun to the galactic center
g – axis inside the galactic plane, perpendicular to c
s – axis pointing into space, perpendicular to c and g
t - time

The ever changing energy inside the Sun is equivalent to a mass effect:

- d/dt(m(c,g,s,t))

The detection of gravitational waves suggests that the changing mass effect can be observed in a distance l, for example in a distance of 150 Million kilometers on Earth:

- $P_{gravitational\_wave}(l,c,g,s,t)$

where $P_{gravitational\_wave}$ denotes the power of a gravitational wave in a distance l of the measurement system from the source, caused by energy outbursts inside the Sun.

Assuming that gravitational waves propagate same as electromagnetic waves with the speed of light, changes of the power distribution inside the Sun become available to the method of interferometry with a baseline b, similar to a well known meridian-transit instrument:

- **$d/dt(E(c,g,s,t)) = f(P_{gravitational\_wave}(l,c,g,s,t),b)$**

The measurement system would consist of multiple measurement points or measurement lines with a mutual distance of chosen baseline b. By interfering the measurement results from all measurement points/lines, an image of the 3-dimensional distribution of energy changes inside the Sun can be estimated.

System considerations

Usually, an instrument for gravitational waves is analyzing phase differences of a laser beam that runs multiple times the distance between an emitter and a reflector before the reflected signal will be brought to interference with the source signal. A gravitational wave will cause a phase change on the traveling laser signal which subsequently will be measured by interfering affected signal with the not-affected laser source signal.

The intended new system is similar in operation to a gravitational wave detector but will take advantage of the relativistic relation between mass and time:

- $t_0/t_f = \text{sqrt}(1 - 2GM/rc^2)$

Above formula expresses the ratio between a local time t_0 passing on the surface of a massive sphere to a coordinate time t_f as passing at an arbitrary far distance:

t_0 – local time on the surface of a spherical object with mass M
t_f – coordinate time at an arbitrary far distance
G – gravitational constant
M – mass of the spherical object
r – radius of the spherical object
c – speed of light

When estimating for example the dilatation on the surface of our Sun this will result in:

- t_0/t_f = sqrt(1 – 2 * 6,6743e-11 * 1,989e30 / (6,96342e8 * 3e8 * 3e8)
- = 0,999997882
- = **-2.118 µs/s**

Thus hypothetically, a precise clock on the surface of our Sun would be delayed by 2.118 µs every second compared to a reference clock at an arbitrary far distance from the Sun.

When taking the relativistic relationship between mass and time into account, gravitational waves can also be considered spacetime waves. Therefore, gravitational waves and also spacetime waves, suggest that our spacetime should be considered an *elastic medium*.

Thus previous interferometry approach to determine the energy change distribution inside our Sun would apply as well to spacetime waves:

- $d/dt\ (E(c,g,s,t) = f(P_{spacetime\_wave}(l,c,g,s,t),b)$

In a practical system setup, a delay line is used to detect changes in the time flow at an observation position on Earth surface:

- $P_{spacetime\_wave} = d(\text{phase}(f) - \text{phase}(f_{delayed}))$

where f is a signal frequency used to detect phase differences between the signal and the delayed signal that results from sending the signal through a delay line.

Above technical implementation of a spacetime wave detector would be able to detect energy outbursts which gradient would exceed the detector's detection threshold:

- **$d/dt\ (E) > F(\ \min(\ d(\text{phase}(f) - \text{phase}(f_{delayed}))))$**

The function F is still subject to be determined theoretically. Nevertheless, a practical system implementation as described in the following will try to deal with the major challenges of spacetime wave detectors which are sensitivity and stability.

The described system will allow to accomplish a sensitivity in the order of 100 ps by a microcontroller based system that is available also to amateurs at low cost of about 150 €.

Spacetime wave detector with Infineon XMC4700 microcontroller

The XMC4700 microcontroller is a versatile industrial device with a high system clock of 144 MHz. An evaluation board of that microcontroller features Arduino connectors what facilitates the implementation of the needed additional electronic circuitry:

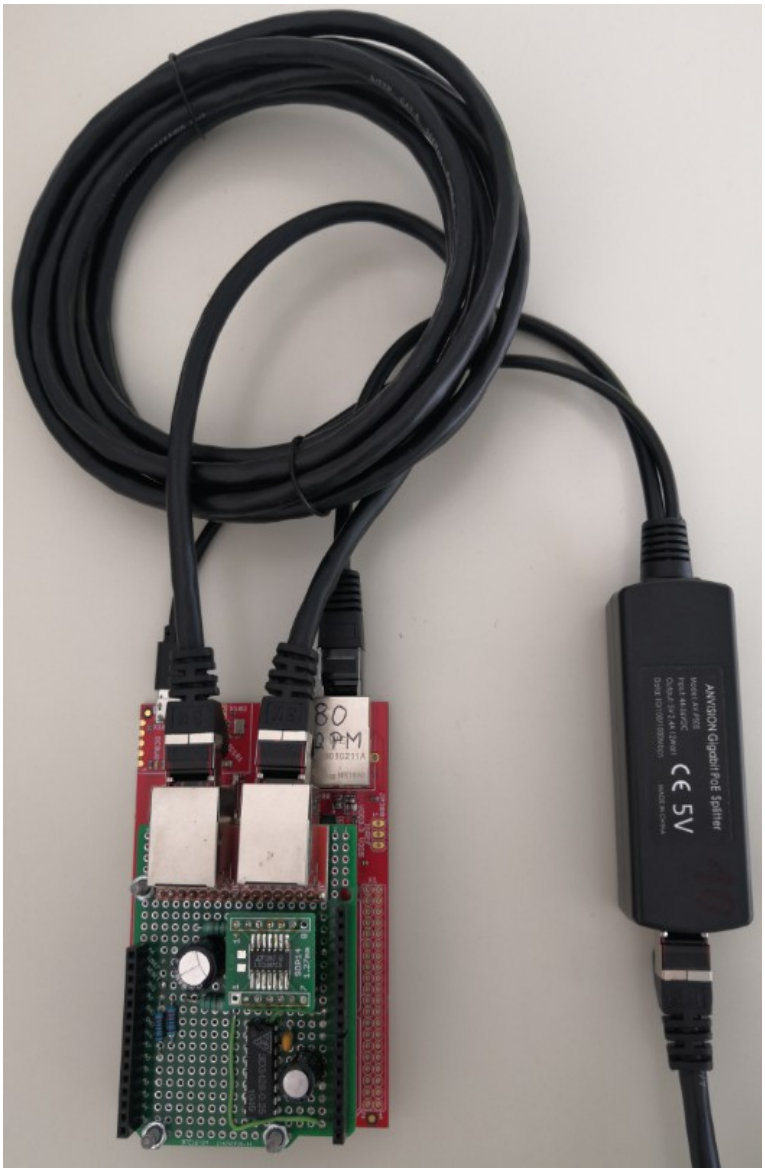

The spacetime wave detector is powered by PoE (power-over-ethernet) from a PoE switch that the device is connected to in an internal network. Two RJ45 sockets are mounted on the Arduino board which connect the pins of the RJ45 network connectors to a LTC1687CS integrated circuit for driving a RS422 line. That IC is connected to the ports of the XMC4700 microcontroller. Furthermore, a 3D3428-0.25 circuit is used to fine-tune the phase shift in steps of about 30 ps.

The delay line consists of a usual network cable which contains four pairs of twisted cable that can be operated as a RS422 line with about 100 Ohm line impedance. One RJ45 connector is working as a reflector which sends the signal back to the other RJ45 connector as it is shown on the layout of the Arduino board. That way the signal travels twice force and back in the network cable before it is converted into a pulse by the RS422 line receiver part of the LTC1687CS circuit.

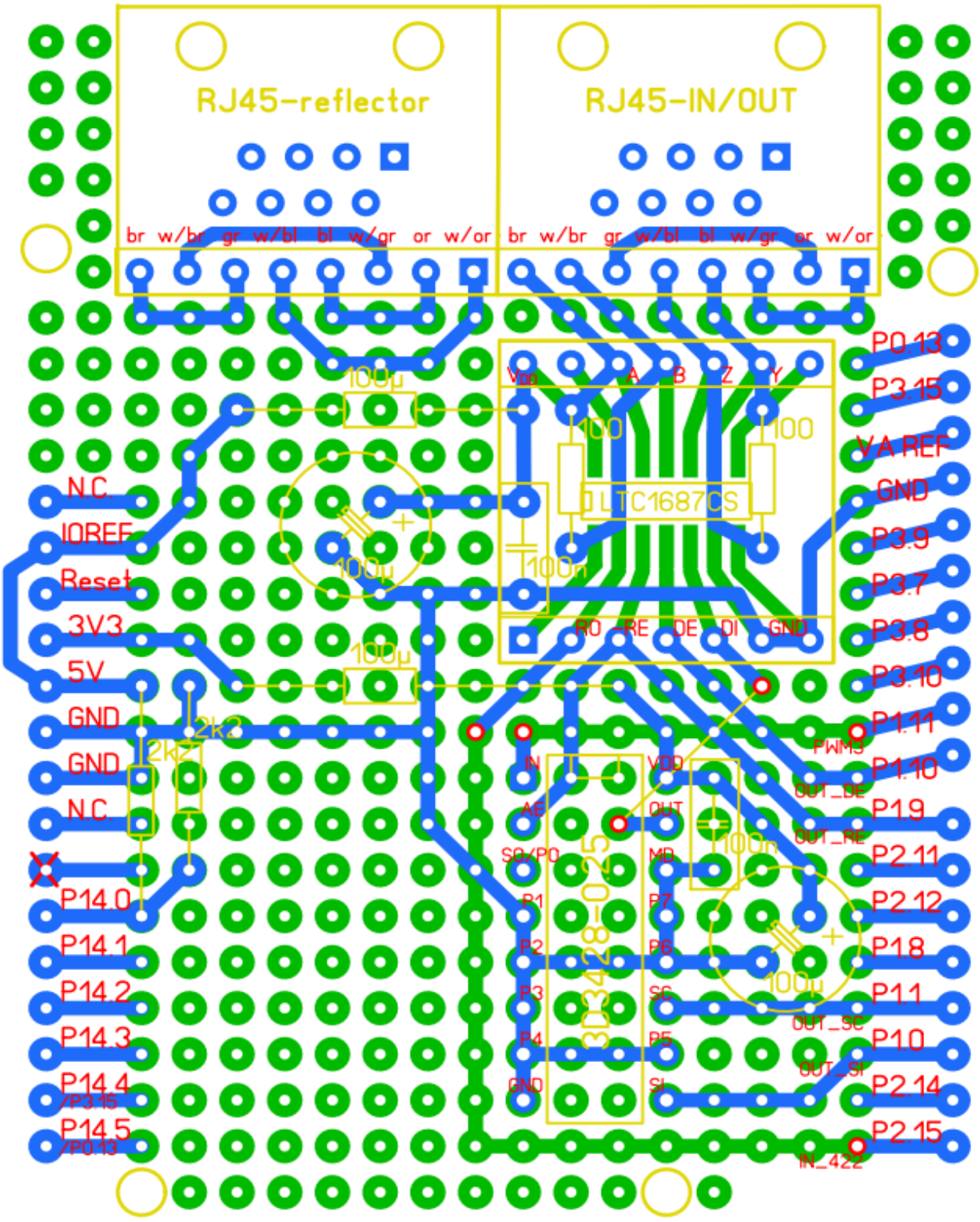

The total distance that the signal travels for example in a 100 m Cat 6a network cable is thus 4 x 100m = 400m. Due to a signal delay of 0.66 inside that cable compared to the speed of light in free space, the equivalent distance would be 600m.

The light needs about 2 µs to travel that distance and thus the signal at the RS422 line receiver is delayed by that value to the signal that is injected by the line driver. The signal that arrives in the microcontroller, however, is delayed by a further offset of about 62 ns due to the signal processing circuitry and due to the logic inside the microcontroller.

Signal processing

The following chart shows the signal run at output from the line receiver (green) which is delayed by one cycle of a 500 kHz signal (2 µs) plus about 300 ns to the signal at output of the line driver (red). The blue line shows the signal according to the RS422 specification at input to the line driver after traveling 400 m through the twisted pair wires of the network cable.

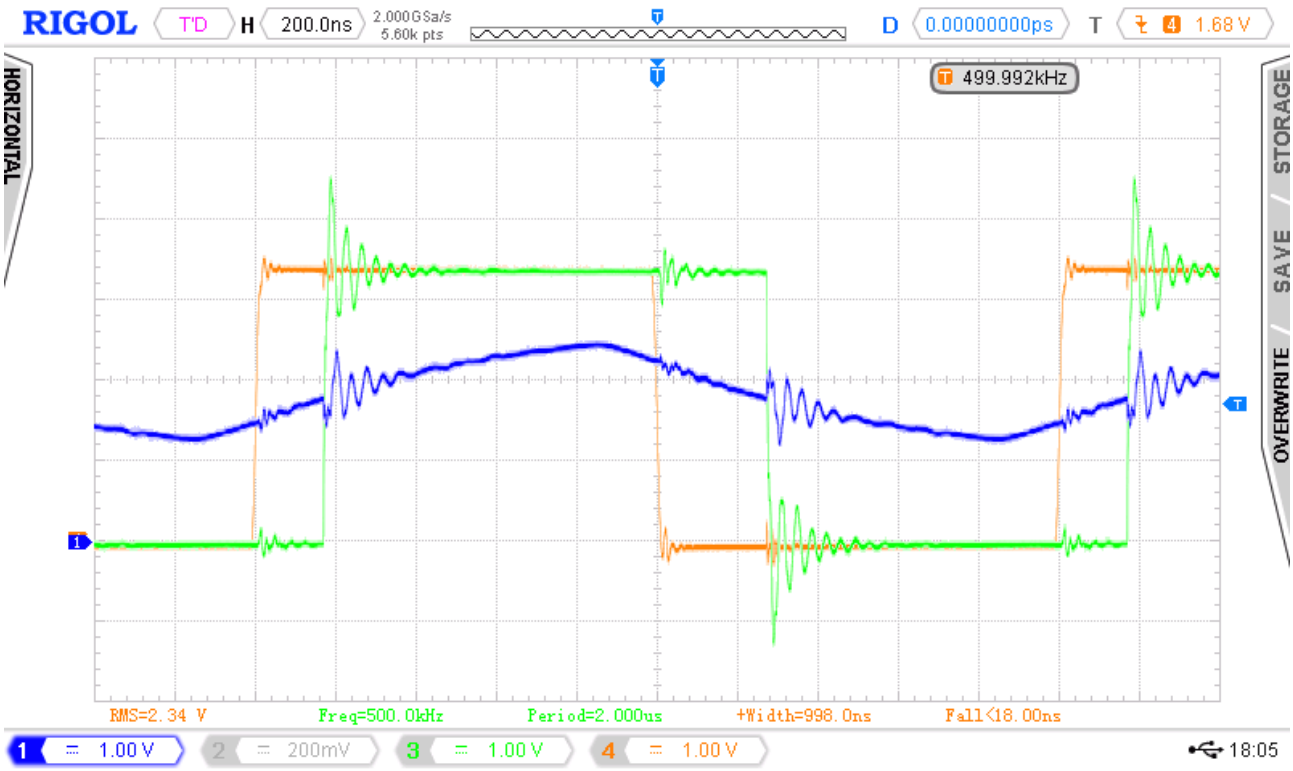

The XMC4700 microcontroller offers a CAPTURE mode which determines the number of clock cycles between start of a pulse from a PWM generator until receiving the delayed signal in the RS422 line receiver.

A clock cycle of 144 MHz as used in the XMC4700 device will result in a granularity of slightly less than 7 ns. That is the base granularity of time with shown electronic circuit.

The granularity of the measurement is improved by adjusting the signal delay such that it is in sync with the edge of the PWM output signal. Ideally, measured delay will then toggle between two values equally. In practice a setup can be accomplished where a series of 1000 measure values contains between 400...600 times the lower respectively the higher delay time. The number of higher values in a 1000 sample measure series will be considered the spacetime wave measure signal.

Whenever the flow of time changes, the sensitive edge discrimination will change and a higher or lower value compared to the average number of high values will result from the change in flow of time. When adjusting the delay line, a deviation of 0.5 ns will cause the spacetime wave measure value to become zero. This means that the granularity of the spacetime wave measurement can be improved by a sensitive edge detection to about 100 ps or better. That offers a detection threshold of about 100 ps/s = **10e-10**.

Required accuracy of delay line adjustment is accomplished by a 3D3428-0.25 that can shift a signal phase by increments of 250 ps. Taking advantage of the 256 delay steps allows to adjust the signal phase even more accurate with a granularity of about 30 ps.

Signal display

The software of the XMC4700 microcontroller runs a web server at standard port 80 on its respective IP address, for example at 192.168.42.51 which last digit is also shown in the title of the signal display.

The signal display draws the raw signal in purple in the Cycle section where a switching between two signal levels should be visible that differ about 7 ns between the bottom and top amplitude values. The number of higher values of those 1000 samples draws one point in green on the Stat section spanning 2 seconds for 800 spacetime wave measure points.

The conversion between the number of high values and the signal delay is based on a LUT (lookup table) that maps numbers from 0..1000 to the respective signal delay, for example to 0..1200 ps with a linear range (red line) between 200 and 800 (=300..900ps).

The bottom part draws 1 / 48 values of those 2-sec-statistics as one point on the Zoom (33min.) / Run (26h) charts. The blue curve shows the highest value and the red curve the lowest value in an interval. The average is shown in black and the green curve (Travel) is a measure of signal variation. The Zoom chart will get zoomed if the signal variation is small.

Automatic adjustment will take place whenever the Monitor (average) leaves 250...750.

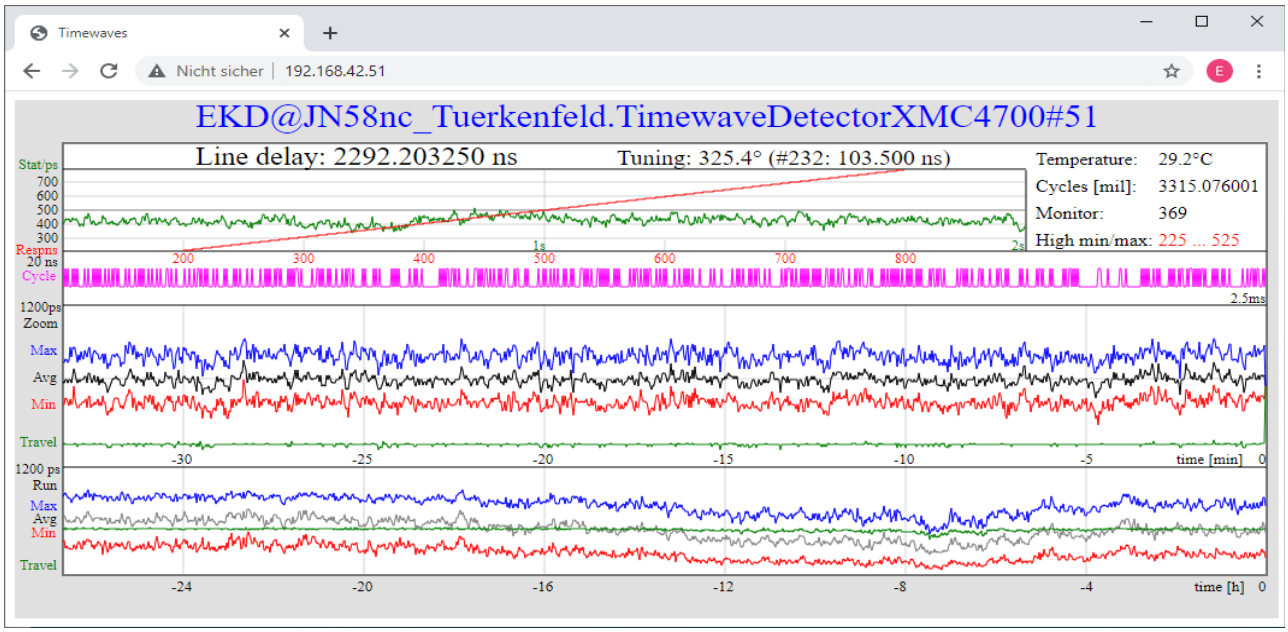

The noise amplitude depends as well on the robustness of the USB supply voltage. Above chart was generated with a PoE splitter that delivers 5V/2A. In case of 500 mA default current of a PC USB port the Stat section may display major distortions due to peak demand for supply current which effects are forwarded also to the Run/Zoom charts.

Therefore, a default 500 mA USB supply should only be used for test/programming purposes. Whenever data quality is on focus, a PoE splitter or an equivalent robust power supply should be used in order to get that interference down to a minimum.

Described solution is working on already mentioned general resolution of about 7 ns / 1000 samples ~= 100 ps at a cycle frequency of 2.5 ms (400 Hz). Along with the statistics over a longer period of e.g. 2 seconds the resolution can be improved further as shown in the Zoom chart of the signal display which may get down to a resolution of 1e-12.

It is important to remember about a stable and robust USB supply for that purpose.

System upgrade in March 2021

Overall resolution was improved based on the consideration that a time flow change would shift the number of higher values up or down. That makes it more likely that the number of subsequent higher or lower values will increase or that the number of subsequent switches between higher and lower values will get higher. A software update implements that idea and monitors both, the maximal number of higher and lower values (called a “pause”) as well as the maximum of subsequent switches between higher and lower values (called a “burst”). That way, the general system resolution was improved to about 10 ps or 1e-11.

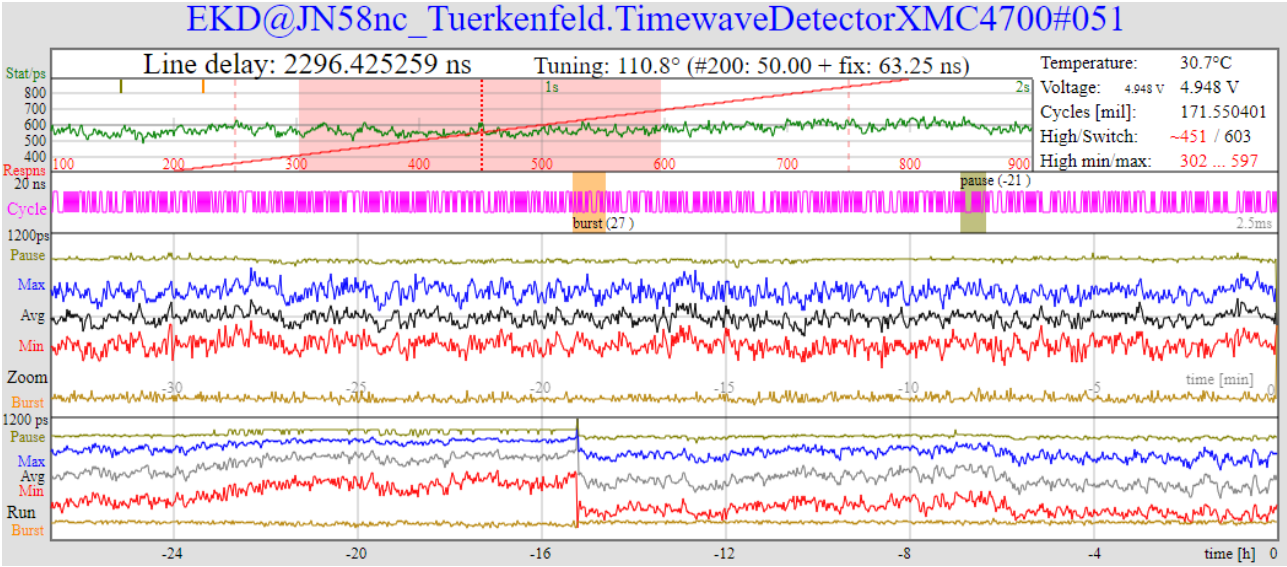

The Cycle part of the display additionally shows positions and lengths of the pause and burst events of maximal length which were determined in past series of 800 cycles. Thus shown ranges do not belong to the displayed cycle which is just the last one of the series.

The positions of pause and burst ranges inside the 800-cycle-series is displayed by small lines in the top of the Stat display. Additionally, the Stat display visualizes the range between lowest and highest number of higher values as well as the operation range of the average high values between 250 and 750. Those ranges as well apply to past 800 cycles.

The long-term charting of the pause and burst signals takes place in the upper part (pause) and the lower part (burst) of the Zoom and the Run display. While the burst signal visualizes higher and lower values of maximal burst length, the pause signal may as well contain jumps. Those jumps are related to detecting the longest pause either on higher or on lower values respectively. A pause on lower values will get negative numbers assigned.

Displayed points of the pause and burst curves related to the appropriate update cycle of those curves which is 2 seconds for the Zoom display and 96 seconds for the Stat display. A re-calibration of the programmed delay line will cause a discontinuity on those displays.

The numeric display in the upper right part of the screen additionally shows the primary supply voltage in the middle of the second row. This might be either about 12 V or 5 V. The second line from bottom of the numeric display displays the average number of higher values followed by the maximal number of switches between higher and lower values inside a 2-second interval which summarizes past 800 cycles of 1000 sample points each.

Once the IP address of a SpacetimeWaveDetector device has been entered in a browser and the first screen was displayed, the screen updates automatically every four seconds.

Observed signals in a predecessor spacetime wave detector system

A previous spacetime wave detector system with a detection threshold of about 10e-9 has been operated by comparing the phases of two 16 MHz oscillators in stable temperature conditions in a distance of about 25 m as it is shown on the following picture:

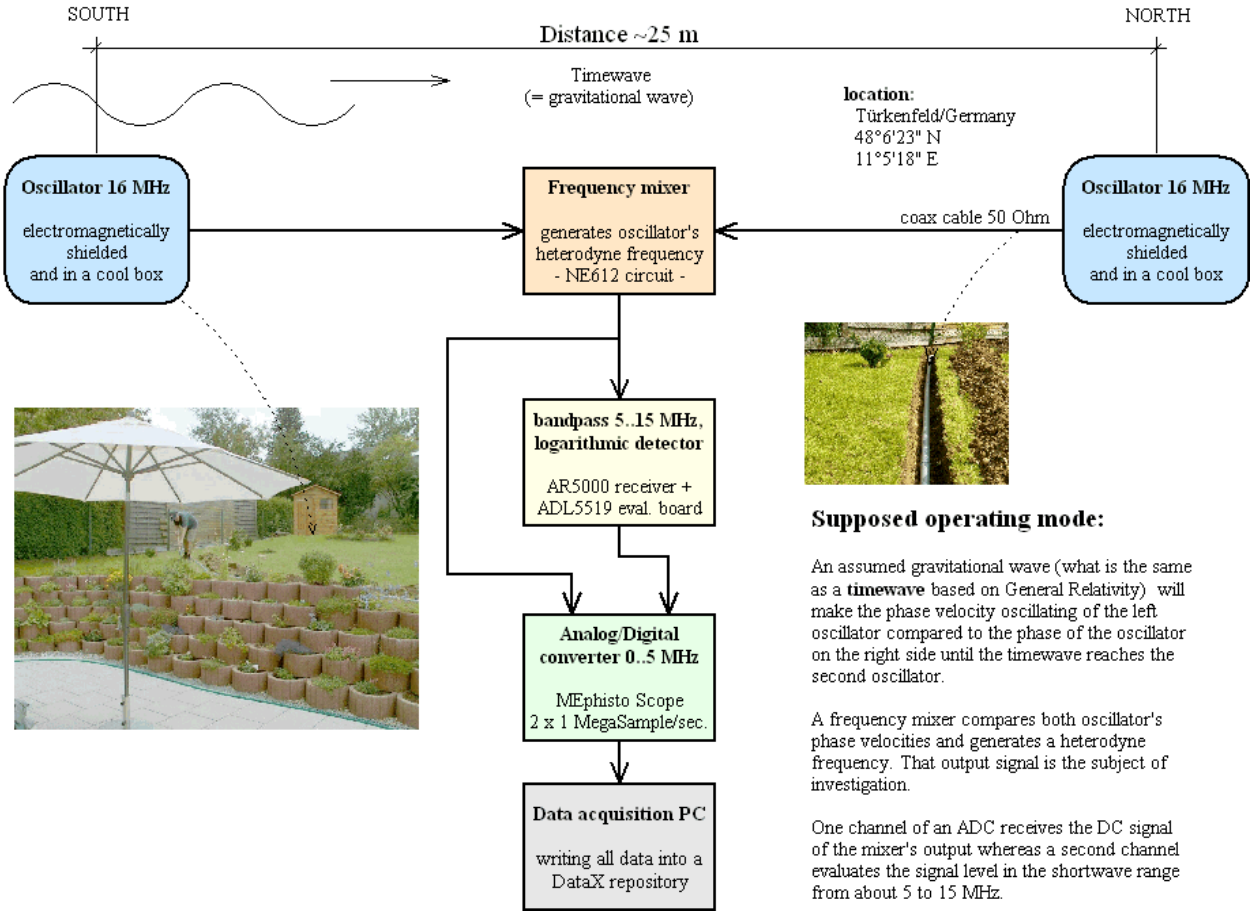

When starting with measurements in mid 2007 it was a challenge to get rid of the various interference signals from electromagnetic devices in the neighborhood. Afterwards, a period of stable signals could be accomplished. Deviations from stable baseline signals could be observed every couple of weeks or months, for example a signal repeating 13 times with a distance of 3604 seconds which also returned some months later:

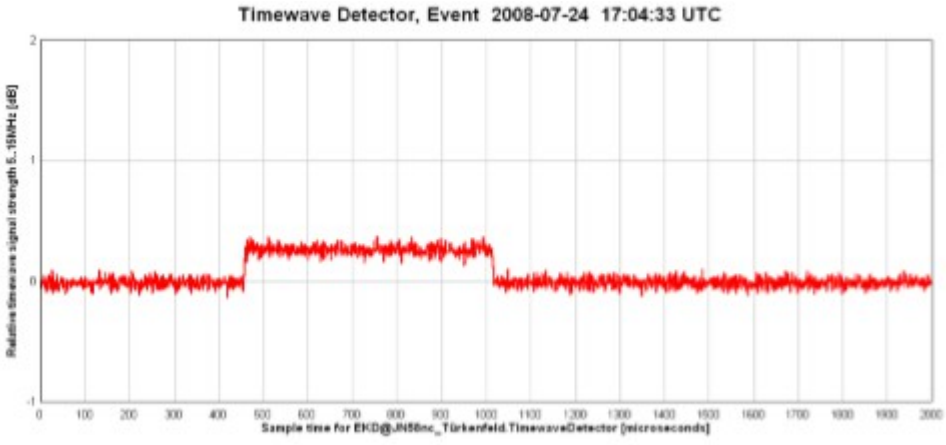

Further measure results are available at https://wegalink.eu/timewaves